AD-A172 649 CONTROL OF ION-VELOCITY DISTRIBUTIONS IN LASER-TARGET 1/1
INTERACTION EXPERIMENTS(U) MISSION RESEARCH CORP
ALBUQUERQUE NM J GRUN ET AL 06 OCT 86 NRL-MR-5652

UNCLASSIFIED F/G 17/8 NL

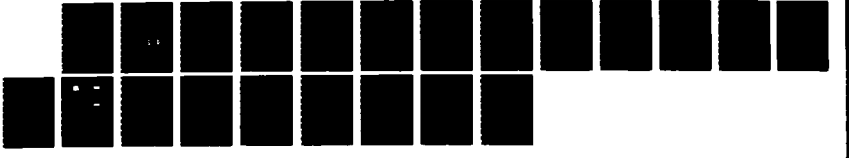

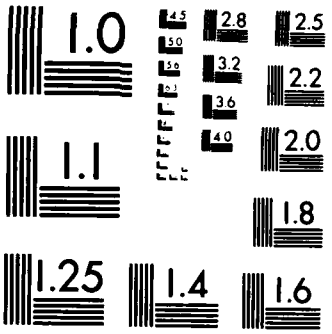

MICROCOPY RESOLUTION TEST CHART
NATIONAL BUREAU OF STANDARDS 1963 A

Naval Research Laboratory

Washington, DC 20375-5000 NRL Memorandum Report 5652 October 6, 1986

Control of Ion-Velocity Distributions in Laser-Target Interaction Experiments

J. GRUN, R. STELLINGWERF* AND B. H. RIPIN

Laser Plasma Branch
Plasma Physics Division

**Mission Research Corporation*
Albuquerque, NM 87106

This work was supported by the Defense Nuclear Agency under Subtask W99QMXWA, work unit 00011 and work unit title "Early Time Experiment," and by the Department of Energy.

AD-A172 649

SECURITY CLASSIFICATION OF THIS PAGE

REPORT DOCUMENTATION PAGE

1a. REPORT SECURITY CLASSIFICATION UNCLASSIFIED	1b. RESTRICTIVE MARKINGS
2a. SECURITY CLASSIFICATION AUTHORITY	3. DISTRIBUTION / AVAILABILITY OF REPORT
2b. DECLASSIFICATION / DOWNGRADING SCHEDULE	Approved for public release; distribution unlimited.
4. PERFORMING ORGANIZATION REPORT NUMBER(S) NRL Memorandum Report 5652	5. MONITORING ORGANIZATION REPORT NUMBER(S)
6a. NAME OF PERFORMING ORGANIZATION Naval Research Laboratory 6b. OFFICE SYMBOL (If applicable) Code 4730	7a. NAME OF MONITORING ORGANIZATION
6c. ADDRESS (City, State, and ZIP Code) Washington, DC 20375-5000	7b. ADDRESS (City, State, and ZIP Code)
8a. NAME OF FUNDING / SPONSORING ORGANIZATION DNA and DOE 8b. OFFICE SYMBOL (If applicable)	9. PROCUREMENT INSTRUMENT IDENTIFICATION NUMBER
8c. ADDRESS (City, State, and ZIP Code) Washington, DC 20305 Washington, DC 20545	10. SOURCE OF FUNDING NUMBERS PROGRAM ELEMENT NO PROJECT NO. AI08-79D P40092 TASK NO. WORK UNIT ACCESSION NO.

11. TITLE (Include Security Classification)

Control of Ion-Velocity Distributions in Laser-Target Interaction Experiments

12. PERSONAL AUTHOR(S)

Grun, J., Stellingwerf, R.* and Ripin, B. H.

13a. TYPE OF REPORT	13b. TIME COVERED	14. DATE OF REPORT (Year, Month, Day)	15. PAGE COUNT
Interim	FROM _____ TO _____	1986 October 6	23

16. SUPPLEMENTARY NOTATION

*Mission Research Corporation, Albuquerque, NM 87106 (Continues)

17. COSATI CODES		
FIELD	GROUP	SUB-GROUP

18. SUBJECT TERMS (Continue on reverse if necessary and identify by block number)

Laser fusion, Fusion, Ions, Plasma, Laser plasma interactions, Ablation

19. ABSTRACT (Continue on reverse if necessary and identify by block number)

The width of ion-velocity distributions from laser-produced plasmas can be controlled experimentally by varying the size of the laser spot. This ion velocity width is determined primarily by whether the ions are mostly in the rarefraction or steady-state regime. It is not dominated by the thermal distribution of the ions, as is often assumed.

20. DISTRIBUTION / AVAILABILITY OF ABSTRACT	21. ABSTRACT SECURITY CLASSIFICATION
☒ UNCLASSIFIED/UNLIMITED ☐ SAME AS RPT. ☐ DTIC USERS	UNCLASSIFIED

22a. NAME OF RESPONSIBLE INDIVIDUAL	22b. TELEPHONE (Include Area Code)	22c. OFFICE SYMBOL
Jacob Grun	(202) 767-2683	Code 4730

DD FORM 1473, 84 MAR 83 APR edition may be used until exhausted. All other editions are obsolete.

SECURITY CLASSIFICATION OF THIS PAGE

16. SUPPLEMENTARY NOTATION (Continued)

This work was supported by the Defense Nuclear Agency under Subtask W99QMXWA, work unit 00011 and work unit title "Early Time Experiment," and by the Department of Energy.

CONTROL OF ION-VELOCITY DISTRIBUTIONS IN LASER-TARGET INTERACTION EXPERIMENTS

The plasma created by a laser beam heating a solid target may be used to provide the thrust for imploding inertial-confinement-fusion pellets[1] or for the acceleration of material for impact and shock wave studies.[2] Laser-produced plasmas are also well suited for studying the coupling and instabilities that occur when an ion beam interacts with a stationary plasma.[3] Such ion beam-plasma interactions occur in many diverse situations such as the aurora, interplanetary shocks, supernova explosions, nuclear detonations in the atmosphere, theta pinch-like devices, and others.[4-6]

A typical ion beam-plasma interaction study requires two component plasmas - a drifting component (the beam) and a stationary component (the background). One way this can be arranged is to have a laser heat a solid target that is placed within an ambient atmosphere.[7-9] The plasma which is generated from the solid target serves as the drifting component and the atmosphere, ionized by radiation from the laser-solid interaction, serves as the background component. In such experiments, it is desirable for both the peak ion velocity and the ion-velocity distribution to be individually controllable and monoenergetic. The mechanisms that control the peak ion velocity have already been analyzed theoretically[10] and experimentally[11] and are well understood: the peak ion speed varies as the 0.2 power of irradiance; it is a weak function of the laser-spot size; and the ion distribution is simple and single-peaked if laser irradiance times the square of the laser wavelength is less than about 10^{14} watts $-\mu m^2/cm^2$.[12]

Manuscript approved January 13, 1986.

However, there has been no experimental attempt at systematic control of the ion-velocity distribution. Many theoretical treatments relate the distribution width to plasma temperature.[13] If temperature is the controlling parameter, then controlling ion-velocity-distributions independently of the peak ion velocity would not be possible.

In this paper, we will demonstrate experimentally that the ion-velocity-distribution width can be controlled and made narrow by varying the laser spot-size. We will show that the distribution width is not controlled by plasma temperature: it is determined primarily by whether the ions are mostly in the rarefraction or the steady-state regime. A simple analytic model relating laser spot-size to ion-distribution width will be developed, and the experiment compared to a code calculation. Our observations and modeling are consistent with the theory of Matzen and Morse who predicted that longer-duration laser pulses produce narrower ion-velocity distributions which they identified as a signature of steady-state flow.[14]

The experiments were performed using the Pharos II laser (1.054 μm wavelength, 4-ns FWHM duration), focused thru f/6 optics onto the surface of foil or disk targets. The resulting irradiation was 10^{12}-10^{13} W/cm^2 which heated the coronal plasma to about 500 eV, causing ions to ablate away from the target at speeds of a few times 10^7 cm/s. Time-of-flight Faraday cups, placed about 27 cm from the targets at 2^o, 17^o, 40^o, and 62^o with respect to the target normal, monitor the ion-current; similarly placed calorimeters monitor the ion energy distribution. Other diagnostics monitor laser energy and duration, and the spatial profile of the laser beam on the target surface. To separate the physics of the initial ion expansion from the physics of any subsequent beam-plasma interaction, we irradiated these targets in vacuum ($<10^{-5}$ Torr).

The widths $\Delta u/u_p$ of the ion-current distribution (FWHM width/peak speed of the Faraday cup peak) were measured as a function of these parameters:

1) Irradiance, which was varied from 1 x 10^{12} to 2.3 x 10^{13} W/cm^2 by changing the laser energy output;
2) Target recoil speed, which was varied from 1/50 to 1/5 of the ablation-ion speed by changing the target's thickness[15]
3) Irradiated-spot size, which was changed in three ways:
   a) by focusing the laser beam and varying the laser energy to produce a variable spot at approximately constant irradiance,
   b) by passing the laser beam thru different diameter apertures placed in the near field,
   c) by irradiating disk targets of different diameter, and,
4) Target composition.

We found that the distribution widths were not sensitive to either irradiance or target speed. They were, however, very sensitive to the size of the irradiated spot, slightly sensitive to target composition for low to moderate-Z materials, and very erratic for high-Z materials.

Figure 1 shows the variation of current-distribution widths of ions from plastic (CH_n) targets as a function of angle and irradiated-spot diameter. It is evident that the width varies as the 0.9 power of the diameter for angles of 40^o or less, i.e., narrow traces are produced by small irradiation diameters. No variation with angle is seen except at 62^o where the widths are significantly broader, peak velocities significantly smaller (200 vs 500 km/s), and no clear correlation with spot size exists. In all cases, broadening of the distribution function is due to an increase of slow

particles in the tail of the Faraday-cup trace. Sample Faraday cup traces are also shown in Figure 1.

The erratic data at 62^{o} can be understood by considering the origin of these ions on the target surface. Previous experiments,[16] have shown that the two-dimensional expansion of plasma from a planar target is similiar to the flow of a nonviscuous, irrotational, incompressible fluid from a circular aperture which is described by Laplace's equation. Therefore, except for (generally small) thermal effects, ions emanating from different points on the target surface are mapped into different asymptotic spatial locations; i.e. each Faraday cup measures ions originating from different regions of the target. Using Laplace's solution, we estimate that the ions at 2^{o}, 17^{o}, and 40^{o} originated from well within the illuminated spot at respective distances of about 0.1, 0.3, 0.7 spot radii from the spot center. The ions at 62^{o}, on the other hand, originate from near the edge of the irradiated spot (about 0.9 radii from the center) where the plasma is cooler and affected by the presence of a target edge. These ions are therefore slower and their velocity spread is larger. Since most of the plasma mass leaves the target at small angles (1/2 of the mass ends up within 40^{o} of the target normal), the ions at 62^{o} constitute a minor fraction of the expanding plasma.

Like the experiment, our hydrodynamic code shows that smaller laser spots produce narrower Faraday cup current traces and ion-velocity distributions. This code, called MACH 1, is one-dimensional in spherical geometry and uses adaptive zoning for good resolution near the critical surface.[17] Laser light absorption is modeled by inverse Bremsstrahlung, which is the dominant absorption mechanism at our irradiances. Multigroup radiation transport and the SESAME equations of state[18] are invoked by the code as necessary.

When matching our experimental results to the code's spherical geometry, we seek to preserve two features: the size of the irradiated spot, and the asymptotic angle θ of the blowoff-plasma expansion. The latter, which is arbitrarily defined as the cone angle that contains half of the total blowoff mass, is found experimentally to be 80^{o}. We require, therefore, that sectors of the code's spherical target that subtend a cone angle of 80^{o} have the same area as that of the illuminated spot. From basic geometry, the appropriate relation is found to be:

$$\pi r_e^2 = 2\pi r_s^2 (1 - \cos(\theta/2)) , \quad (1)$$

where r_e and r_s are the illuminated spot and sphere radii respectively. For $\theta = 80^{o}$ $r_s = 1.5\ r_e$. The code, using spherical targets of this radius and of the same thickness and composition as in the experiment, runs for the entire laser pulse duration, after which time the ion-velocity distribution does not change significantly. The blowoff plasma is then "collected" to simulate the action of the Faraday cup.

We produced simulated Faraday cup traces and ion velocity distributions corresponding to two shots in our experiment - one where a target was irradiated with a small (200 μm) diameter spot and another with a larger (700μ m) diameter spot. These are shown in Figs. 2a and 2c. Note that the current traces and velocity distributions for the two cases are very different, even though the peak velocities and plasma temperatures are similiar. The corresponding profiles of ion-velocity versus distance profiles from the target, at the peak of the laser pulse, are shown in Fig. 2b. The code predicts that the width of the ion-velocity distributions varies as the 1.15

power of the focal irradiation diameter (Fig. 3) - very close to the 0.9 power measured in the experiment. The code also predicts that the ion distribution width scales linearly with laser wavelength. The laser wavelength, however, was fixed in our experiment so that this prediction is not yet verified.

We can derive analytically a relationship between laser-spot-size and ion-velocity profile width. Consider two very simplified analytic descriptions of the blowoff expansion process; namely the solution which describes the rarefaction caused by a sudden planar expansion of an isothermal gas:[19]

$$v=(r-r_s)/t + c \tag{2a}$$

$$n=n_s e^{-v/c}, \tag{2b}$$

and the isothermal wind solution that describes the steady-state, spherical expansion of a gas:[20]

$$0.5(v/c)^2 - \ln(v/c) = 2\ln(r/r_s) + 0.5 \tag{3a}$$

$$nvr^2 = \text{constant}. \tag{3b}$$

Here, v and c are the plasma and sound speeds; and r, r_s stand for distance and target radius respectively; n is the density and t is time. Looking at Figure 2b again, it is apparent that the steady-state velocity solution (dotted line) is similiar in shape to the code prediction for a small spot; whereas the

transient-state rarefaction solution (dashed line) is closer to the prediction for a larger spot. Since the steady-state solution is "flatter" than the rarefaction solution we intuitively expect that its velocity distribution and current traces would be more monoenergetic; i.e. narrower. We reason, therefore, that if during most of the laser pulse the flow is characterized by the rarefaction solution, the velocity distributions will be broad. If, on the other hand, the solution crosses over to steady-state early in the laser pulse, the velocity distributions will tend to be narrower.

The plasma flow can, in the above simplified view, be described by a combination of these two ideal solutions - with the outer edge of the flow (i.e. the ions that left the target early) following the rarefaction solution, and the inner part of the flow (i.e. the ions that left the target later) following the wind solution. The crossover from the rarefaction to the wind solutions will occur while the laser pulse is still on if the velocities given by Eq. 2 and Eq. 3 are equal at some time $t \leq \tau$, the laser pulse duration. Substituting Eq. 2 with $t \equiv \tau$ into Eq. 3 we get the expression for the cross-over point,

$$0.5Q^2 - \ln(Q) - 2\ln(r_i/r_s) - 0.5 = 0 \tag{4}$$

where,

$$Q = (r_s/c\tau)(r_i/r_s - 1) + 1.$$

Thus, the normalized radius at crossover, r_i/r_s, is a function of $r_s/c\tau$ only. If $r_s/c\tau$ is small, the crossover occurs at large r_i/r_s so that most of the ion flow is governed by the steady state wind solution and we would predict narrow ion-velocity distributions. Otherwise,

the cross-over occurs nearer to the target so that most of the flow is not in steady state and hence we predict broader temporal ion-velocity distributions. This relationship between $r_s/c\tau$, the flow solutions, and the ion-velocity widths is consistent with experimental observations. For example, the narrowest Faraday cup distribution at 40 degrees or less has a width ($\Delta u/u_p$) of 0.1 and the broadest 0.6. The corresponding values of $r_s/c\tau$ are estimated to be 0.1 and 0.5 . Thus, the ion-velocity distribution shapes depend primarily on the geometry of the experiment. Longer pulses will provide narrower distributions as predicted by Matzen and Morse.[14]

In addition to plastic targets, we also irradiated aluminium, nickel, silver, and gold foils. We observed two types of behavior: For atomic numbers up through nickel, the Faraday-cup traces exhibited the same single-peaked velocity distribution that was seen in plastic targets. The distribution width, however, did increase slightly with atomic number. For example, nickel targets irradiated with a 810 μm diameter laser spot had a distribution width ($\Delta u/u_p$) of 0.75 ($\pm$ 0.05) while similarly irradiated plastic targets had a width of 0.6 (+0.05,-0.1). Aluminium distribution widths fell in between at 0.65 ($\pm$ 0.05). The silver and gold targets behaved quite differently: The ion distributions were very broad and so multi-peaked that a unique definition of width was no longer possible.

One may argue that the small amount of broadening of single peaked distributions with increasing atomic number occurs because higher atomic number plasmas take longer to reach steady state. This is because the sound speed is lowered by radiation cooling and by a decreasing contribution of the ion-pressure term. However, this argument does not consider charge distributions within the plasma and associated effects such as charge

exhange. It also does not explain the very different behaviour of the silver and gold foils. Since our diagnostics do not distinguish different charge states, little else can be said on this topic. It is nevertheless encouraging that the major correlations that we observe can be explained by rather simple physics.

One subtle point is worth mentioning. When the irradiation diameter is varied, not only the spot-size but also the spatial profile of the irradiation changes somewhat. Consequently, there is no entirely precise definition of "irradiation diameter," especially when comparing different methods of spot size variation. However, since the biggest variations are in the low intensity edge of the profile, we can define a practical spot-size by ignoring the wings of the irradiance distribution. Because of this, the experimental irradiation diameter is defined as the lesser of the spot diameter that contains 50% of the energy, or the diameter of the irradiated disk when the target is not a wide foil. This convention is consistent with the code model's treatment of the ablation plasma in the forward 80° sector of the target. If one were to choose a definition of spot size that was more sensitive to the tail of the irradiation profile (such as the spot that contains 90% of the energy), then all the qualitative effects described above would still hold, but the absolute scaling parameters would depend on the method used to vary the spot-size.

Another point to keep in mind is that at any point in space and time the instantaneous velocity spread is negligible in both the steady-state and rarefaction regimes. Rather, the ion-velocity sweeps through the range measured by the Faraday-cup current width - the fastest ions first and slower ions later in time

In conclusion, we have demonstrated that it is possible to systematically control the width of velocity distributions of ablation plasma from laser-irradiated targets and to create very narrow distributions. Since the distribution width is not a sensitive function of irradiance, but the peak speed is, both these quantities may be controlled individually. This should make it easier to do cleaner beam-plasma interaction experiments and, consequently, better comparison to theory. We point out that the widths of the ion-velocity distributions in laser-target interaction experiments are not primarily determined by temperature, as is assumed in many analytic treatments. Rather our results and theoretical modeling suggest that the width of the distribution is proportional to sound transit time thru the plasma divided by the laser pulse duration in agreement with the theoretical work of Matzen and Morse.[14] To obtain the narrowest ion velocity distributions, one should use small, low Z targets with short wavelength, longer duration laser pulses.

The authors thank Dr. Charles Manka for many stimulating conversations. This work was supported by the Defense Nuclear Agency and the Department of Energy.

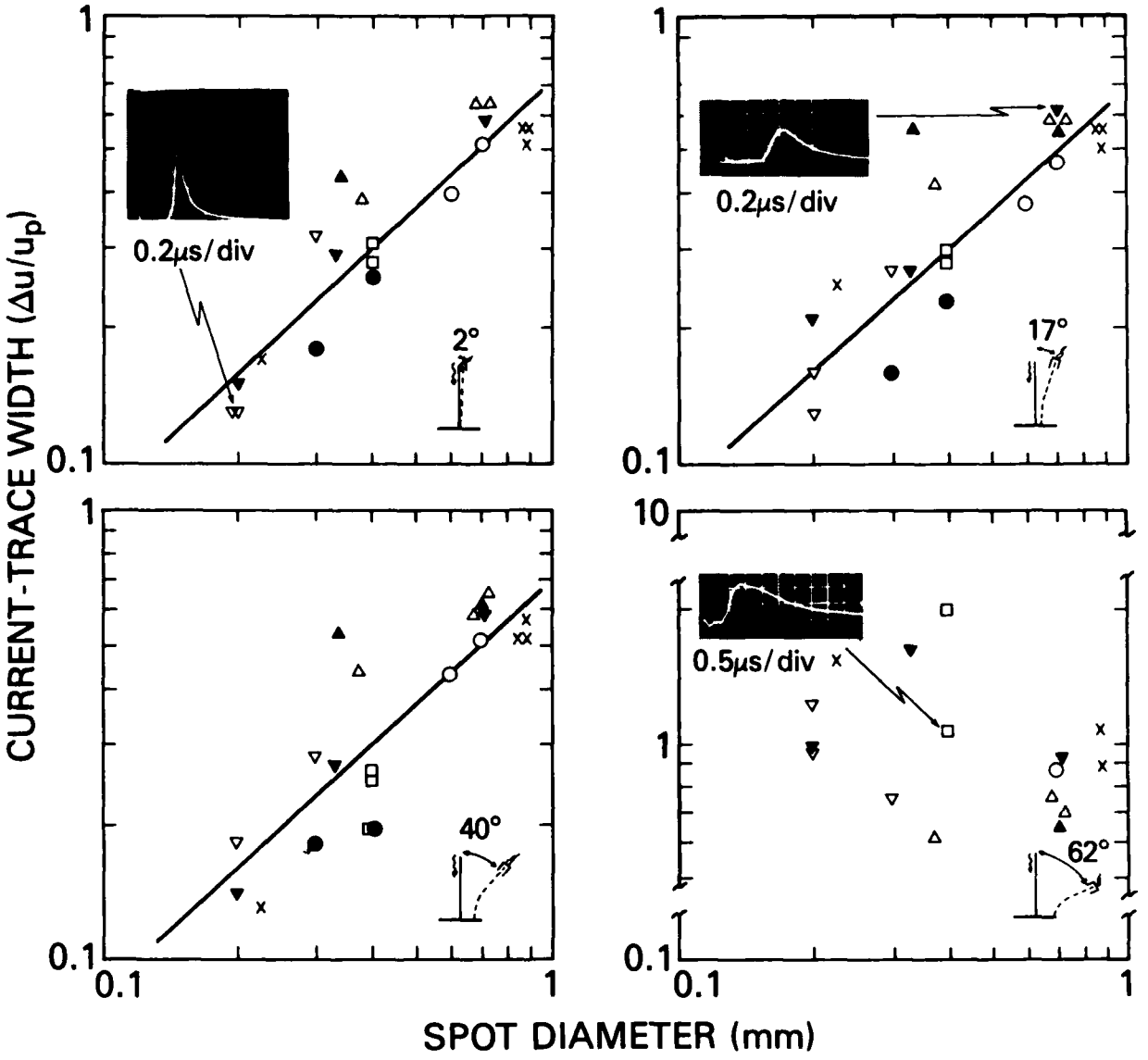

FIGURE 1. Current trace width ($\Delta u/u_p$) versus irradiated spot diameter at 2, 17, 40 and 62 degrees to the target normal. Symbols indicate the method used to vary spotsize: Δ, ▲- aperturing the laser beam; ▼ - focusing beam on foil target; ∇ focusing beam on disk target; 0, ●- changing size of disk target; x - not part of any of the above sequences. Squares indicate variation in irradiance (1-6 x 10^{12}). Insets show typical Faraday-cup traces.

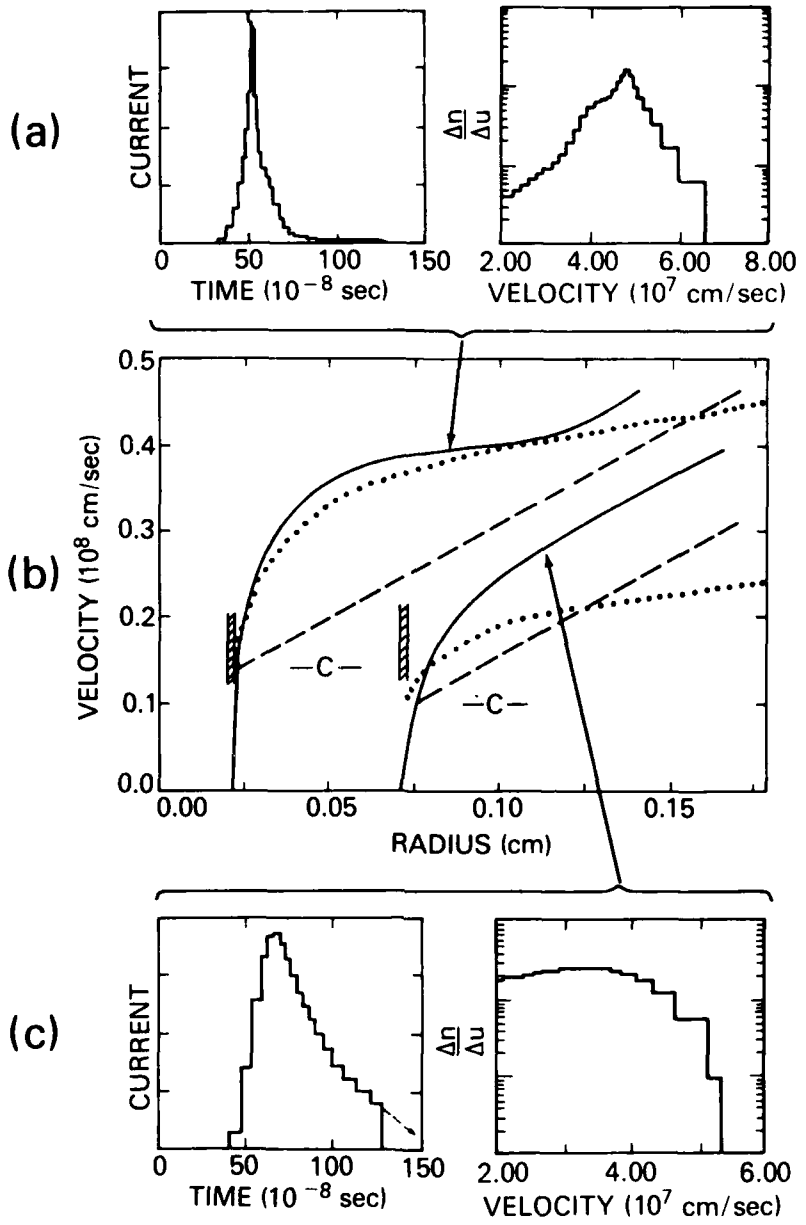

FIGURE 2. Theoretical results: (a) Computer-generated Faraday cup trace and ion-velocity distribution for a plastic target irradiated with 3.5 x 10^{12} W/cm^2 in a 200-μm spot and [(c)] a plastic target irradiated with 1.4 x 10^{12} W/cm^{2}in a 700-μm spot. (b) Velocity profiles at the peak of the laser pulse versus radius calculated with the code (solid line), with the steady-state spherical solution (dotted line), and the planar rarefaction expansion solution (dashed line). Aproximate sound speed in the blowoff plasma is indicated by a "C".

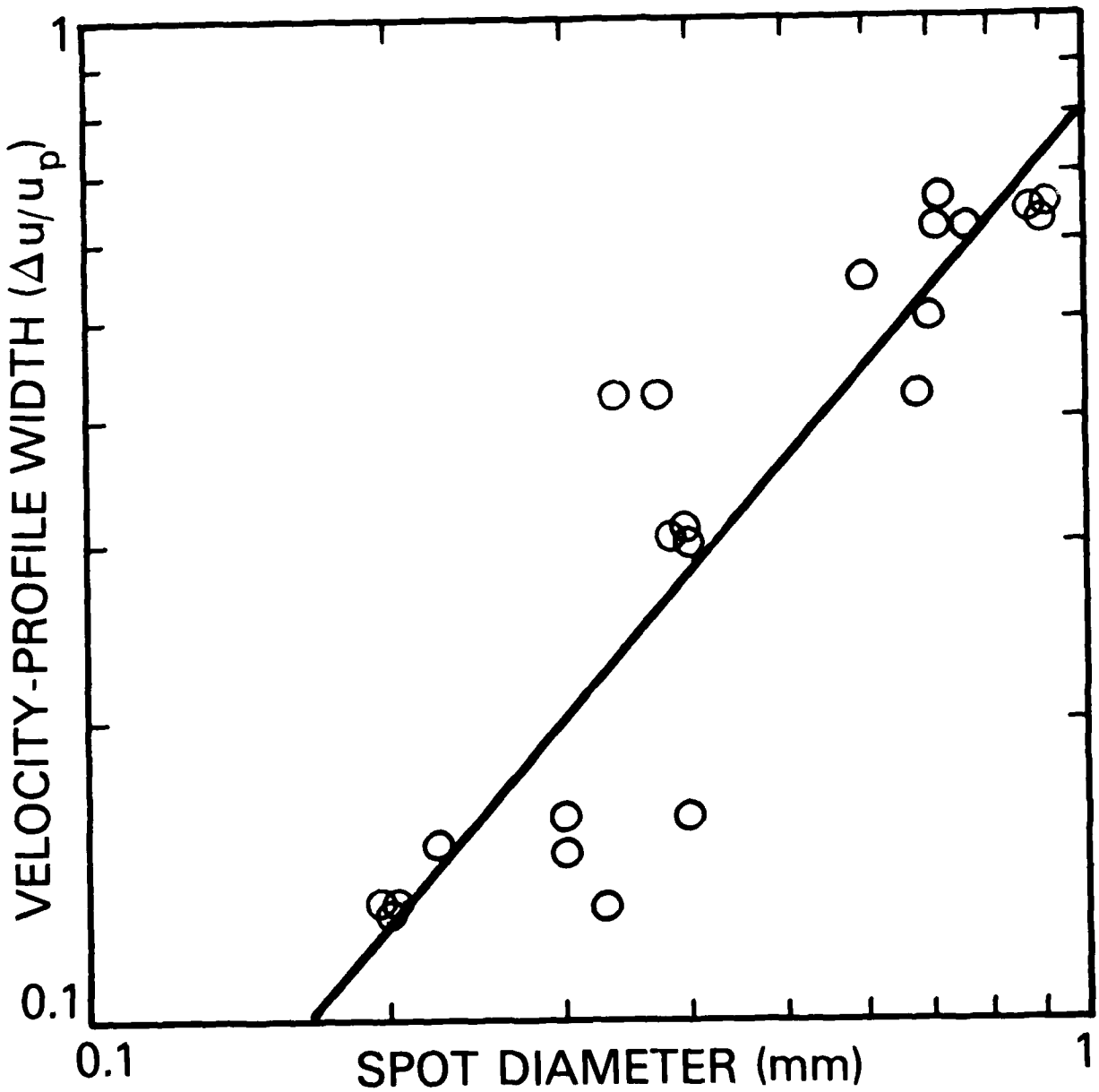

FIGURE 3. Widths of ion-current traces predicted by the code for our shots and a least-squares fit to the results.

REFERENCES

1. J. Nuckolls, L. Wood, A. Thiessen, and G. Zimmerman, Nature 239, 139 (1972).

2. J. Grun, S.P. Obenschain, B..H. Ripin, R.R. Whitlock, E.A. McLean, J. Gardner, M.J. Herbst, and J.A. Stamper, Phys. Fluids 26, 588 (1983).

3. A. Hasegawa, Plasma Instabilities and Nonlinear Effects, Springer-Verlag, NY (1975).

4. Solar-Terrestrial Influences on Weather and Climate, B.M. McCormac, T.A. Seliga, eds., D. Reidel, Boston (1979).

5. J.W. Chamberlain, Physics of the Aurora and Airglow, Academic Press, New York (1961).

6. The Effects of Nuclear Weapons, S. Glasstone and P.J. Dolan, eds., U.S. Department of Defense and The Energy Research and Development Adm., Washington, D.C. (1977). (AD-A087 568)

7. S.O. Dean, E.A. McLean, J.A. Stamper, and H.R. Griem, Phys. Rev. Letters 27, 487 (1971).

8. D.W. Koopman, Phys. Fluids 15, 1959 (1972); A.Y. Cheung, R.R. Goforth, and D.W. Koopman, Phys. Rev. Letters 31, 429 (1973); D.W. Koopman and R.R. Goforth, Phys. Fluids 17, 1560 (1974); G. Jellison and C.R. Parsons, Phys. Fluids 26, 1171 (1983).

9. B.H. Ripin, A.W. Ali, H. Griem, J. Grun, S. Kacenjar, C.K. Manka, E.A. McLean, A.M. Mostovych, S.P. Obenschain, and J.A. Stamper in Laser Interactions and Related Plasma Phenomena, Volume 7, H. Hora and G. Miley, eds., Plenum Press (1986)

10. Yu. V. Afanasyev, O.N. Krokhin, and G.V. Sklizkov, IEEE Journal of Quantum Electronics QE-2, 483 (1966); R.E. Kidder,Nuclear Fusion 8, 3 (1968); A. Caruso, and R. Gratton, Plasma Physics 10, 867 (1968); T.R. Jarboe, W.B. Kunkel, and A.F. Lietzke, Phys. Fluids 19, 1501 (1976); S.J. Gitomer, R.L. Morse, and B.S. Newberger, Phys. Fluids 20, 234 (1977); C.E. Max, C.F. McKee, and W.C. Mead, Phys. Fluids 23, 1620 (1980).

11. H. Opower, W. Kaiser, H. Puell, and W. Heinicke, Z. Naturforschg, 22, 1392 (1967); J. Grun, S.P. Obenschain, B.H. Ripin, R.R. Whitlock, E.A. McLean, J. Gardner, M.J. Herbst, and J.A. Stamper, Phys. Fluids 26, 588 (1983); J.P. Anthes and M.K. Matzen, J. Appl. Phys. 54, 3438 (1983); M.H. Key, W.T. Toner, T.J. Goldsack, J.D. Kilkenny, S.A. Veats, P.F. Cunningham, and C.L.S. Lewis, Phys. Fluids 26, 2011 (1983); P.D. Gupta, P.A. Naik, and H.C. Pant, Appl. Phys. Lett. 43, 754 (1983); B. Meyer and G. Thiell, Phys. Fluids 27, 302 (1984).

12. J. Grun, R. Decoste, B.H. Ripin, and J. Gardner,Appl. Phys. Lett. 39, 545 (1981).

13. I. Gorog, Phys. Lett. 28A, 371 (1968); N. Inoue, Y. Kawasumi, and K. Miyamoto, Plasma Phys. 13, 84 (1970); H. Kang, T. Yamanaka, K. Yoshida, M. Waki, and C. Yamanaka, Japan J. Appl. Phys. 11, 765 (1972); N.G. Utterback, S.P. Tang and J.F. Friichtenicht, Phys. Fluids 19, 900 (1976); R.H. Hughes, R.J. Anderson, C.K. Manka, M.R. Carruth, L.G. Gray, and P.J. Rosenfeld, J. Appl. Phys. 51, 4088 (1980).

14. M.K. Matzen and R.L. Morse, Phys. Fluids 22, 654 (1979).

15. These were plastic (CH_n) foils, 3-20 μm thick, that were irradiated at $2x10^{12}$ W/cm^2. Their speeds were not measured in this experiment. However, based on previous experiments and code calculations we estimate that their speed varied from 10-100km/sec which is respectively 1/50 to 1/5 of the measured ablation-ion speed.

16. M.J. Herbst and J. Grun, Phys. Fluids 24, 1917 (1981).

17. M. Alme, M. Frese, R. Stellingwerf, Mission Research Corporation Report AMRC-R-486 (1984) [to be submitted to PACS]. (AD A156 030)

18. This is a tabular equation of state maintained by and available from the Los Alamos National Laboratory (We used the 1985 version of the tables).

19. Ya. B. Zel'dovich, Yu. P. Raizer, Physics of Shock Waves and High Temperature Hydrodynamic Phenomena, Academic Press, NY (1966), pg. 33-38, pg.101-106.

20. J.C. Brandt, Introduction to the Solar Wind, W.H. Freeman, San Francisco (1970), pg. 63-66.

Distribution List

Lawrence Livermore National Lab.
P.O. Box 808
Livermore, CA 94551
Dr. W. Kruer, L-545
Dr. B. Lasinski, L-32
Dr. J. Lindl, L-32
Dr. C. Max, L-545
Dr. V. Rupert, L-13
Dr. D. Phillion
Dr. W. Mead
Dr. R. More
Dr. N. Ceglio
Dr. R. Kidder
Dr. E.M. Campbell
Dr. R.P. Drake
Dr. R.L. Kauffman
Dr. R. Lee
Dr. D.L. Matthews
Dr. R.E. Turner
Dr. F. Ze
Dr. C.A. Anderson
Dr. M. Tabak
Dr. L. Suter, L-477
Dr. M.D. Rosen
Dr. K. Mikaelian
Dr. J. Mark, L-477
Dr. T.R. Dittrich, L-23
Dr. S. Hatchett, L-477
Dr. R.H. Price, L-473
Dr. D. Bailey, L-477

KMS Fusion
3941 Research Park Drive
Post Office Box 1567
Ann Arbor, MI 48106
Dr. F. Mayer
Dr. R. Johnson
Dr. R Berger
Dr. T. Spieziali
Dr. D. Slater

Mission Research Corporation
P.O. Box 719
Santa Barbara, CA 93120
Dr. C. Longmire

Larry L. Altgilbers
3805 Jamestown
Huntsville, AL 35810

Maxwell Labs
8835 Balboa Ave.
San Diego, CA 92123
M. Gersten
J. Riordin

Los Alamos National Laboratory
P.O. Box 1663
Los Alamos , NM 87544
Dr. D. Forslund
Dr. S. Gitomer
Dr. J. Kindel
Dr. C. Elliot
Dr. D. Giovanelli
Dr. T. Tan
Dr. G. Kyrala
Dr. S. Singer
Dr. P. Goldstone
Dr. W. Ehler
Dr. A.H. Williams
Dr. L. Burkhardt
Dr. D. Erickson
Dr. D. Thomson

University of Maryland
Dept. of Physics & Astronomy
College Park, MD 20740
Dr. C. Liu
Dr. E. Ott
Dr. H. Griem

University of Rochester
Laboratory for Laser Energetics
Rochester, NY 14627
Dr. B. Yaakobi
Dr. J. Soures
Dr. M. Richardson
Dr. S. Craxton
Dr. E. Thorsos
Dr. W. Seka
Dr. S. Skupsky
Dr. K. Tanaka
Dr. J. Delettrez

Sandia National Laboratory
P.O. Box 5800
Albuquerque, NM 87185
Dr. F.C. Perry
Dr. M. Widnor
Dr. J. Olson
Dr. D.L. Hanson

University of California
Department of Applied Science
Davis, CA 95616
J.S. DeGroot

David Pirkle
404-L Eagle Heights Apts.
Madison, WI 53705

Dennis Manos
P.O. Box 451
Princeton Plasma Physicvs Lab
Princeton, NJ 08544

Department of the Army
Harry Diamond Laboratory
2800 Powder Mill Road
Adelphi, MD 20783
Dr. H.E. Brandt

A. Ng
Physics Department
U.B.C.
2075 Wesbrook Mall
Vancouver, B.C.
CANADA

Fons Masswinkel
MPI fur Quantenoptik'D8046
Garching
FRG

M. Roccella
Associazione Euratom-CNEN Fusione
Frascati, Roma, Italy

CEA
Centre d'etudes de Limiel
BP-27, 94190 Villevenue St. Georges
France
B. Duborgel
D. Billone
T. Plantevin

Institut fur Plasmaphysik
8046 Garching
Bei Munchen
West Germany
Dr. R. Sigel
Dr. K. Eidmann
Dr. A.G.M. Maaswinkel

National Research Council
Division of Physics
100 Susser Drive
Ottawa K1A-OR6, Canada
Dr. J. Alcock
Dr. N. Burnett
Dr. G. Lougheed

University of Quebec
INRS Energie
Case Postale 1020
Varennes, Quebec
Dr. T. Johnson
Dr. R. Decoste
Dr. H. Pepin

Laboratorie de Physique des
Milieuz Ionises
Ecole Polytechnique
17, Rue Descartes
75230 Paris Cedex 05
FRANCE
Dr. E. Fabre
Dr. J. Virmont

Institute for Laser Engineering
Osaka University
Suita Osaka, 565, JAPAN
Dr. C. Yamanaka
Dr. S. Hakai
Dr. T. Mochizuki
Dr. Y. Izawa
Dr. M. Matoba
Dr. T. Yabe
Dr. K. Nishihara
Dr. K. Mima
Dr.H. Azechi
Dr. T. Yamanaka

Soreq Nuclear Center
Yavne, ISRAEL
Dr. A. Krumbein
Dr. H. Zmore
Dr. S. Jackel
Dr. B. Arad
Dr. H. Loebenstein
Dr. S. Eliezer

END

11-86

DTIC